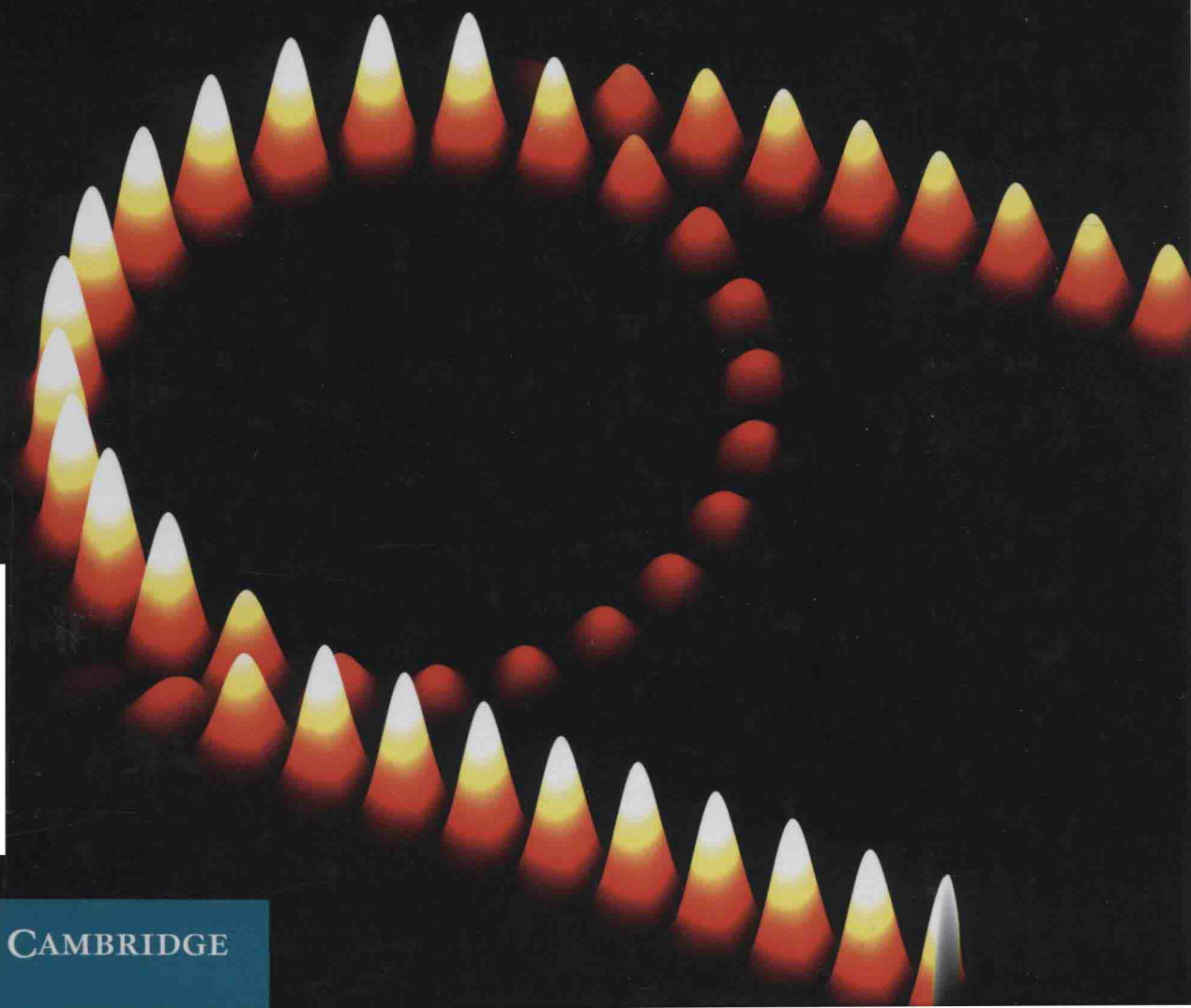


EuMA

EuMA HIGH FREQUENCY TECHNOLOGIES SERIES

Plasmonic Nanoelectronics and Sensing

ER-PING LI and HONG-SON CHU



CAMBRIDGE

Plasmonic Nanoelectronics and Sensing

ER-PING LI and HONG-SON CHU

A*STAR Institute of High Performance Computing, Singapore



CAMBRIDGE
UNIVERSITY PRESS

CAMBRIDGE
UNIVERSITY PRESS

University Printing House, Cambridge CB2 8BS, United Kingdom

Published in the United States of America by Cambridge University Press, New York

Cambridge University Press is a part of the University of Cambridge.

It furthers the University's mission by disseminating knowledge in the pursuit of education, learning and research at the highest international levels of excellence.

www.cambridge.org

Information on this title: www.cambridge.org/9781107027022

© Cambridge University Press 2014

This publication is in copyright. Subject to statutory exception and to the provisions of relevant collective licensing agreements, no reproduction of any part may take place without the written permission of Cambridge University Press.

First published 2014

Printed in the United Kingdom by TJ International Ltd. Padstow Cornwall

A catalogue record for this publication is available from the British Library

ISBN 978-1-107-02702-2 Hardback

Cambridge University Press has no responsibility for the persistence or accuracy of URLs for external or third-party Internet websites referred to in this publication, and does not guarantee that any content on such websites is, or will remain, accurate or appropriate.

Plasmonic Nanoelectronics and Sensing

Plasmonic nanostructures provide new ways of manipulating the flow of light, with nanostructures and nanoparticles exhibiting optical properties never before seen in the macro-world. Covering plasmonic technology from fundamental theory to real-world applications, this work provides a comprehensive overview of the field.

- Discusses the fundamental theory of plasmonics, enabling a deeper understanding of plasmonic technology
- Details numerical methods for modeling, design, and optimization of plasmonic nanostructures
- Includes step-by-step design guidelines for active and passive plasmonic devices, demonstrating the implementation of real devices in the standard CMOS nanoscale electronic–photonic integrated circuit to help cut design, fabrication, and characterization time and cost
- Includes real-world case studies of plasmonic devices and sensors, explaining the benefits and downsides of different nanophotonic integrated circuits and sensing platforms.

Ideal for researchers, engineers, and graduate students in the fields of nanophotonics and nanoelectronics as well as optical biosensing.

Er-Ping Li is a Principal Scientist and Director of Nanophotonics and Electronics at the Institute of High Performance Computing, A*STAR, Singapore. He is a Fellow of the IEEE and of the Electromagnetics Academy, USA.

Hong-Son Chu is a Scientist at the Nanophotonics and Electronics Department of the Institute of High Performance Computing, A*STAR, Singapore. He is a member of the Optical Society of America, the IEEE, and the Materials Research Society.

EuMA High Frequency Technologies Series

Series Editor

Peter Russer, Technical University of Munich

Homayoun Nikookar, *Wavelet Radio*

Thomas Zwick, Werner Wiesbeck, Jens Timmermann, and Grzegorz Adamiuk (Eds),
Ultra-wideband RF System Engineering

Er-Ping Li and Hong-Son Chu, *Plasmonic Nanoelectronics and Sensing*

Forthcoming

Peter Russer, Johannes Russer, Uwe Siart, and Andreas Cangellaris, *Interference and Noise in Electromagnetics*

Maurizio Bozzi, Apostolos Georgiadis, and Ke Wu, *Substrate Integrated Waveguides*

Luca Roselli (Ed.), *Green RFID Systems*

George Deligeorgis, *Graphene Device Engineering*

Luca Pierantoni and Fabio Coccetti, *Radiofrequency Nanoelectronics Engineering*

Alexander Yarovoy, *Introduction to UWB Wireless Technology and Applications*

Contributors

1 Fundamentals of plasmonics and

2 Plasmonic properties of metal nanostructures

Yuriy A. Akimov

*A*STAR Institute of High Performance Computing, Singapore*

3 Frequency-domain methods for modeling plasmonics

Zhengdong Liu

*A*STAR Institute of High Performance Computing, Singapore*

4 Time-domain simulation for plasmonic devices

Iftikhar Ahmed and Eng Huat Khoo

*A*STAR Institute of High Performance Computing, Singapore*

6 Silicon-based active plasmonic devices for on-chip integration

Dim-Lee Kwong, Guo-Qiang Lo, and Shiyang Zhu

*A*STAR Institute of Microelectronics, Singapore*

7 Plasmonic biosensing devices and systems

Lin Wu and Ping Bai

*A*STAR Institute of High Performance Computing, Singapore*

Preface

Data communication and information processing are driving the rapid development of ultra-high speed and ultra-compactness in nano-photo-electronic integration. Plasmonics technology has in recent years demonstrated the promise to overcome the size mismatch between microscale photonic and nanoscale electronic integration, and it likely will be crucial for the next generation of on-chip optical nano-interconnects, enabling the deployment of small-footprint and low-energy integrated circuitry.

The phenomenon of surface plasmons was first observed in the Lycurgus cup, which is a Roman glass cage cup in the British Museum, London, UK. This special cup is made of a dichroic glass that shows a different color depending on the condition of illumination. Specifically, in daylight, the cup appears to have a green color, which means that light is being reflected from the cup; however, when a light is shone into the cup and transmitted through the glass, it appears to have a red color. Today, we know that this fascinating behavior is due to nanoscopic-scale gold and silver particles embedded in the glass. However, it took 1500 years and doubtless countless fantastic interpretations for a plausible explanation to emerge. In the last few decades, the phenomenon of surface plasmons has been extensively studied both theoretically and experimentally, and there have been attempts to use it for various applications ranging from solar-cell energy and sensing to nanophotonic devices.

This book presents the results from many years of our collective research in the fields of nanoplasmonics and its applications. It presents state-of-the-art plasmonics device modeling and design techniques, with novel developments in particular in CMOS-compatible integrated circuits and sensing technologies. We hope this book can serve as a good basis for further progress in this field, both in academic research and for industrial applications. The book consists of seven chapters, contributed by Yuriy Akimov, Zhengtong Liu, Iftikhar Ahmed, Eng Huat Khoo, Er-Ping Li, Hong-Son Chu, Wu Lin, and Bai Ping, from the Department of Electronics and Photonics, Institute of High Performance Computing, Singapore, and Shiyang Zhu, Patrick Guo-Qiang Lo, and Dim-Lee Kwong from the Institute of Microelectronics, Agency for Science Technology and Research, Singapore.

Chapter 1 introduces the fundamentals of plasmonics associated with Maxwell's theory and applications in plasmonics. Chapter 2 provides an introduction to the plasmonic properties of metal nanostructures. Chapter 3 presents the modeling and simulation of plasmonics associated with plasmonic devices by implementation of frequency-domain numerical methods. In Chapter 4, time-domain simulation methods, in

particular the finite-difference time-domain method, are introduced for passive and active plasmonic device design. Chapter 5 describes the development of various passive plasmonic waveguides, in particular CMOS-compatible devices for on-chip nanoelectronic integration, and Chapter 6 presents CMOS-compatible active plasmonic devices for on-chip nanoelectronic integration. Both theoretical studies and experimental results are presented in these two chapters. The recent development of plasmonics for biosensing applications is presented in Chapter 7.

We gratefully acknowledge the research support from the Agency for Science Technology and Research, Singapore. Also acknowledged are the contributors to the book, Drs. Yuriy Akmov, Zhengtong Liu, Iftikhar Ahmed, Eng Huat Khoo, Wu Lin, Bai Ping, Shiyang Zhu, and Patrick Guo-Qiang Lo and Professor Dim-Lee Kwong, who did the really hard work. We also wish to express our gratitude to Mia Balashova and Julie Lancashire from Cambridge University Press for their great assistance in keeping us on schedule. Finally, we are grateful to all the contributors' families, without whose continuing support and understanding this book would never have been published.

We hope that this book will serve as a valuable reference for engineers, researchers, and post-graduate students in the fields of nanophotonics and nanoelectronics as well as optical biosensing. Even though much has been accomplished in these fields, we predict that many more exciting challenges will arise in these areas.

Er-Ping LI and Hong-Son CHU

Contents

	<i>List of contributors</i>	page ix
	<i>Preface</i>	xi
1	Fundamentals of plasmonics	1
1.1	Electromagnetic field equations	1
1.1.1	Maxwell's equations in a medium	1
1.1.2	Material equations	2
1.1.3	Temporal and spatial dispersion in metals	4
1.2	The local-response approximation	6
1.2.1	The energy of an electromagnetic field in metals	6
1.2.2	Properties of the complex dielectric permittivity	7
1.2.3	The conduction-electron contribution	8
1.2.4	The bound-charge contribution	10
1.3	Electromagnetic fields in metals	14
1.3.1	Plasmon classification	14
1.3.2	Bulk plasmon modes	17
1.3.3	Surface plasmon modes	18
	References	19
2	Plasmonic properties of metal nanostructures	20
2.1	Plasmonic modes in spherical geometry	20
2.1.1	Spherical harmonics	20
2.1.2	Electromagnetic fields in vector spherical harmonics	22
2.1.3	Spherical plasmons	23
2.1.4	Scattering by a sphere	26
2.1.5	Cross-sections	28
2.1.6	A multilayer sphere	32
2.2	Plasmonic modes in cylindrical geometry	35
2.2.1	Cylindrical harmonics	35
2.2.2	Electromagnetic fields in vector cylindrical harmonics	36
2.2.3	Cylindrical plasmon polaritons	38
2.2.4	Scattering by a cylinder	40
2.2.5	Cross-sections per unit length	43
2.2.6	Multilayer cylinder	46

2.3	Plasmonic modes in planar geometry	49
2.3.1	Planar harmonics	50
2.3.2	Electromagnetic fields in vector planar harmonics	51
2.3.3	Planar plasmon polaritons	52
2.3.4	Reflection and transmission by a slab	56
2.3.5	Reflectance, transmittance, and absorptance	58
2.3.6	A multilayer slab	60
	References	65
3	Frequency-domain methods for modeling plasmonics	67
3.1	Introduction	67
3.2	Rigorous coupled-wave analysis	68
3.2.1	Formulations	68
3.2.2	Modeling 2D and 3D plasmonic nanostructures with RCWA	79
3.3	A semi-analytical method for near-field coupling study	87
3.3.1	Superlens and subwavelength imaging	87
3.3.2	Object–superlens coupling	87
3.4	Summary	95
	References	95
4	Time-domain simulation for plasmonic devices	99
4.1	Introduction	99
4.2	Formulation	101
4.2.1	A model for metals	101
4.2.2	A model for solid-state materials	107
4.2.3	Simulation of an MSM waveguide and a microcavity	111
4.2.4	SPP generation using an MSM microdisk	114
4.3	Surface plasmon generation in semiconductor devices	120
4.4	Implementation of the LD model on a GPU	125
4.4.1	GPU implementation	127
4.4.2	Applications	130
4.5	Summary	134
	References	135
5	Passive plasmonic waveguide-based devices	139
5.1	Introduction	139
5.2	The vertical hybrid Ag–SiO ₂ –Si plasmonic waveguide and devices based on it	142
5.2.1	Theoretical background	142
5.2.2	The dependence of the propagation characteristics on the thickness of the SiO ₂ stripe	143

5.2.3	The dependence of the propagation characteristics on the dimensions of the Si nanowire	144
5.2.4	The propagation characteristics of the vertical hybrid, metal–insulator–metal, and dielectric-loaded plasmonic waveguides	147
5.2.5	Waveguide couplers	149
5.2.6	Waveguide bends	151
5.2.7	Power splitters	153
5.2.8	Ring resonator filters	155
5.3	Complementary metal–oxide–semiconductor compatible hybrid plasmonic waveguide devices	159
5.3.1	CMOS-compatible plasmonic materials	160
5.3.2	Vertical hybrid Cu–SiO ₂ –Si plasmonic waveguide devices	161
5.3.3	Horizontal hybrid Cu–SiO ₂ –Si–SiO ₂ –Cu plasmonic waveguide devices	165
	References	176
6	Silicon-based active plasmonic devices for on-chip integration	180
6.1	Introduction	180
6.2	Plasmonic modulators based on horizontal MISIM plasmonic waveguides	182
6.2.1	The operating principle	182
6.2.2	Experimental demonstration	186
6.2.3	Issues and possible solutions	189
6.3	Athermal ring modulators based on vertical metal–insulator–Si hybrid plasmonic waveguides	191
6.3.1	Device structure	191
6.3.2	Device properties	192
6.3.3	Tolerance	200
6.4	Schottky-barrier plasmonic detectors	201
6.4.1	Device structure	201
6.4.2	SPP power absorption	202
6.4.3	Quantum efficiency	204
6.4.4	Dark current and speed	207
6.5	Metallic nanoparticle-based detectors	208
6.5.1	Device structure	208
6.5.2	LSPR-enhanced absorption	208
6.5.3	Experimental demonstration	210
6.5.4	Issues and solutions	212
6.6	Conclusions	213
	References	214

7	Plasmonic biosensing devices and systems	217
7.1	Introduction	217
7.2	Plasmonic sensing mechanisms	219
7.2.1	Resonance conditions for sensing	219
7.2.2	Sensitivity and figure of merit	220
7.3	Plasmonic biosensing systems	222
7.3.1	Sensor structures	222
7.3.2	Modulation methods	226
7.3.3	Bio-functionalization formats	227
7.4	Design methods	228
7.4.1	The N -layer model	228
7.4.2	The FEM model	229
7.5	Plasmonic biosensor design examples	233
7.5.1	Graphene-based biosensor design	233
7.5.2	Messenger RNA detection	237
7.5.3	Point-of-care clinical screening of PSA	241
	References	247
	<i>Index</i>	249

1 Fundamentals of plasmonics

In this chapter, we give a brief introduction to the classical electrodynamics of metals that constitutes the basis of modern plasmonics. We review the Maxwell equations for electromagnetic fields and consider the main optical properties of metals within the local-response approximation. In conclusion, we give a general classification of plasmons that appear in metal structures.

1.1 Electromagnetic field equations

1.1.1 Maxwell's equations in a medium

Most of the electromagnetic phenomena occurring in metals are well described within the classical electrodynamics based on the *macroscopic Maxwell equations*. These equations assume the use of the statistically averaged (over an ensemble of the equivalent systems) electric and magnetic fields. Practically, the averaging is performed in space over “physically small” volumes, which are much smaller than the wavelength, but much longer than the mean interatomic distance. Within this approach, we neglect all field fluctuations that occur at atomic scales and consider only the macroscopic response of the medium.

In the absence of external charges and currents, the macroscopic Maxwell equations for electromagnetic fields in a medium can be written as follows:¹

$$\nabla \times \mathbf{E} = -\frac{1}{c} \frac{\partial \mathbf{B}}{\partial t}, \quad \nabla \cdot \mathbf{E} = 4\pi\rho, \quad (1.1)$$

$$\nabla \times \mathbf{B} = \frac{1}{c} \frac{\partial \mathbf{E}}{\partial t} + \frac{4\pi}{c} \mathbf{j}, \quad \nabla \cdot \mathbf{B} = 0, \quad (1.2)$$

where \mathbf{E} is the electric field, \mathbf{B} is the magnetic induction, ρ is the induced internal charge density, \mathbf{j} is the induced electric current density, and c is the speed of light in vacuum. The induced charges and currents comprise the medium's response to the electromagnetic field, as a result of its polarization and magnetization.

¹ Throughout this chapter, all quantities and equations are written in the Gaussian unit system for a more natural description of electromagnetic fields. For conversion to the SI unit system, we refer the reader to the textbook by Jackson [1].

In general, the induced charges and currents are given with the *polarization* \mathbf{P} and *magnetization* \mathbf{M} fields,

$$\rho = -\nabla \cdot \mathbf{P}, \quad (1.3)$$

$$\mathbf{j} = \frac{\partial \mathbf{P}}{\partial t} + c \nabla \times \mathbf{M}, \quad (1.4)$$

that allow us to rewrite the macroscopic Maxwell equations in a simpler form,

$$\nabla \times \mathbf{E} = -\frac{1}{c} \frac{\partial \mathbf{B}}{\partial t}, \quad \nabla \cdot \mathbf{D} = 0, \quad (1.5)$$

$$\nabla \times \mathbf{H} = \frac{1}{c} \frac{\partial \mathbf{D}}{\partial t}, \quad \nabla \cdot \mathbf{B} = 0, \quad (1.6)$$

where \mathbf{D} and \mathbf{H} are the auxiliary fields called the electric displacement and magnetic field, which are introduced to account for the polarization and magnetization of the medium,

$$\mathbf{D} = \mathbf{E} + 4\pi \mathbf{P}, \quad (1.7)$$

$$\mathbf{H} = \mathbf{B} - 4\pi \mathbf{M}. \quad (1.8)$$

Thus, the Maxwell equations in a medium give us the relation between two pairs of electric $\{\mathbf{E}, \mathbf{D}\}$ and magnetic $\{\mathbf{B}, \mathbf{H}\}$ fields. In this sense, Eqs. (1.5) and (1.6) do not form a closed set of equations until we provide *material relations* for the medium's response to electric and magnetic fields. In general, these relations are given by field-dependent functions for polarization $\mathbf{P} = \mathbf{P}(\mathbf{E})$ and magnetization $\mathbf{M} = \mathbf{M}(\mathbf{B})$ vectors that eventually result in material relations for the auxiliary fields $\mathbf{D} = \mathbf{D}(\mathbf{E})$ and $\mathbf{H} = \mathbf{H}(\mathbf{B})$.

1.1.2 Material equations

Establishing the relations for $\mathbf{D}(\mathbf{E})$ and $\mathbf{H}(\mathbf{B})$ is the key issue, since it describes how the medium responds to electromagnetic fields. In general, these relations are non-linear. However, for \mathbf{E} and \mathbf{B} fields that are not too high, the auxiliary fields $\mathbf{D}(\mathbf{E})$ and $\mathbf{H}(\mathbf{B})$ can be approximated with linear functions. This is the so-called *linear-electrodynamics* approach. In this approximation, the response of the medium at a given point \mathbf{r} and moment t is assumed to be a linear function of electromagnetic fields at any point \mathbf{r}' taken at all preceding moments $t' < t$ in accordance with the causality principle,

$$D_i(t, \mathbf{r}) = \int_{-\infty}^t dt' \int d\mathbf{r}' \varepsilon_{ij}(t, t', \mathbf{r}, \mathbf{r}') E_j(t', \mathbf{r}'), \quad (1.9)$$

$$B_i(t, \mathbf{r}) = \int_{-\infty}^t dt' \int d\mathbf{r}' \mu_{ij}(t, t', \mathbf{r}, \mathbf{r}') H_j(t', \mathbf{r}'). \quad (1.10)$$

Note that here we write the dependence $\mathbf{B}(\mathbf{H})$ instead of $\mathbf{H}(\mathbf{B})$. It is caused by the symmetry of Maxwell's equations observed with respect to the field pairs $\{\mathbf{E}, \mathbf{D}\}$ and

$\{\mathbf{H}, \mathbf{B}\}$. Following this symmetry, it is more natural to consider the dependence $\mathbf{B}(\mathbf{H})$, rather than $\mathbf{H}(\mathbf{B})$. For this reason, the field \mathbf{H} is commonly called the magnetic field, by analogy with the electric field \mathbf{E} , although it is actually an auxiliary quantity.

The functions $\varepsilon_{ij}(t, t', \mathbf{r}, \mathbf{r}')$ and $\mu_{ij}(t, t', \mathbf{r}, \mathbf{r}')$ in Eqs. (1.9) and (1.10) characterize the efficiency of the material response transfer from one point of space and time to another. For a medium that is homogeneous in space and time, the functions ε_{ij} and μ_{ij} depend on the differences $t - t'$ and $\mathbf{r} - \mathbf{r}'$. In this case,

$$D_i(t, \mathbf{r}) = \int_{-\infty}^t dt' \int d\mathbf{r}' \varepsilon_{ij}(t - t', \mathbf{r} - \mathbf{r}') E_j(t', \mathbf{r}'), \quad (1.11)$$

$$B_i(t, \mathbf{r}) = \int_{-\infty}^t dt' \int d\mathbf{r}' \mu_{ij}(t - t', \mathbf{r} - \mathbf{r}') H_j(t', \mathbf{r}'). \quad (1.12)$$

By performing the Fourier transform,

$$G(t, \mathbf{r}) = \frac{1}{(2\pi)^2} \iint G(\omega, \mathbf{k}) e^{i(\mathbf{k} \cdot \mathbf{r} - \omega t)} d\omega d\mathbf{k},$$

of D_i , E_j , B_i , and H_j in the (t, \mathbf{r}) space, we get the material relations for the fields in the frequency-wavevector space (ω, \mathbf{k}) ,

$$D_i(\omega, \mathbf{k}) = \varepsilon_{ij}(\omega, \mathbf{k}) E_j(\omega, \mathbf{k}), \quad (1.13)$$

$$B_i(\omega, \mathbf{k}) = \mu_{ij}(\omega, \mathbf{k}) H_j(\omega, \mathbf{k}). \quad (1.14)$$

Here, $\varepsilon_{ij}(\omega, \mathbf{k})$ and $\mu_{ij}(\omega, \mathbf{k})$ are the tensors of complex permittivity and permeability given by

$$\varepsilon_{ij}(\omega, \mathbf{k}) = \int_0^\infty dt_1 \int d\mathbf{r}_1 \varepsilon_{ij}(t_1, \mathbf{r}_1) e^{-i(\mathbf{k} \cdot \mathbf{r}_1 - \omega t_1)}, \quad (1.15)$$

$$\mu_{ij}(\omega, \mathbf{k}) = \int_0^\infty dt_1 \int d\mathbf{r}_1 \mu_{ij}(t_1, \mathbf{r}_1) e^{-i(\mathbf{k} \cdot \mathbf{r}_1 - \omega t_1)}, \quad (1.16)$$

where $t_1 = t - t'$ and $\mathbf{r}_1 = \mathbf{r} - \mathbf{r}'$.

For an isotropic medium, the properties of which are identical in any direction, $\varepsilon_{ij}(\omega, \mathbf{k})$ and $\mu_{ij}(\omega, \mathbf{k})$ can be composed of the unit tensor δ_{ij} and the tensor $k_i k_j$, since they are the only two tensors of second rank formed from the vector \mathbf{k} . In this case, we have

$$\varepsilon_{ij}(\omega, \mathbf{k}) = \left(\delta_{ij} - \frac{k_i k_j}{k^2} \right) \varepsilon_t(\omega, \mathbf{k}) + \frac{k_i k_j}{k^2} \varepsilon_l(\omega, \mathbf{k}), \quad (1.17)$$

$$\mu_{ij}(\omega, \mathbf{k}) = \left(\delta_{ij} - \frac{k_i k_j}{k^2} \right) \mu_t(\omega, \mathbf{k}) + \frac{k_i k_j}{k^2} \mu_l(\omega, \mathbf{k}). \quad (1.18)$$

Thus, among the nine components of each tensor ε_{ij} and μ_{ij} , only two components are independent, namely $\varepsilon_t(\omega, \mathbf{k})$ and $\varepsilon_l(\omega, \mathbf{k})$ for ε_{ij} , and $\mu_t(\omega, \mathbf{k})$ and $\mu_l(\omega, \mathbf{k})$ for μ_{ij} . The

meaning of those components becomes clear if we write \mathbf{D} and \mathbf{B} in vector form,

$$\begin{aligned}\mathbf{D}(\omega, \mathbf{k}) &= \varepsilon_l(\omega, \mathbf{k}) \frac{\mathbf{k} \times (\mathbf{E} \times \mathbf{k})}{k^2} + \varepsilon_l(\omega, \mathbf{k}) \frac{\mathbf{k}(\mathbf{E} \cdot \mathbf{k})}{k^2}, \\ \mathbf{B}(\omega, \mathbf{k}) &= \mu_l(\omega, \mathbf{k}) \frac{\mathbf{k} \times (\mathbf{H} \times \mathbf{k})}{k^2} + \mu_l(\omega, \mathbf{k}) \frac{\mathbf{k}(\mathbf{H} \cdot \mathbf{k})}{k^2}.\end{aligned}$$

According to these expressions, $\varepsilon_l(\omega, \mathbf{k})$ and $\mu_l(\omega, \mathbf{k})$ give the medium response to longitudinal electric ($\mathbf{E} \times \mathbf{k} = 0$) and magnetic ($\mathbf{H} \times \mathbf{k} = 0$) fields, while $\varepsilon_t(\omega, \mathbf{k})$ and $\mu_t(\omega, \mathbf{k})$ describe the response to transverse electric ($\mathbf{E} \cdot \mathbf{k} = 0$) and magnetic ($\mathbf{H} \cdot \mathbf{k} = 0$) fields.

1.1.3 Temporal and spatial dispersion in metals

In the general case, both tensors ε_{ij} and μ_{ij} depend on the frequency ω and the wavevector \mathbf{k} . Eventually, any electromagnetic pulse disperses by propagating in the medium, as the Fourier components

$$G(\omega, \mathbf{k})e^{i(\mathbf{k} \cdot \mathbf{r} - \omega t)}$$

with different ω and \mathbf{k} (that comprise the pulse in accordance with the Fourier transform) propagate with different phase velocities ω/k . Thus, materials with properties that exhibit frequency and wavevector dependence are *dispersive*. The frequency dependence of the tensors ε_{ij} and μ_{ij} describes the *temporal dispersion* of electromagnetic fields, while the wavevector dependence gives the *spatial dispersion*.

In the optical range, metals feature very strong temporal dispersion. It arises due to the inertia and friction of electrons in metals that make the polarization and magnetization inertial with respect to electric and magnetic fields. Thus, the metal's response at a given moment t is dependent on the values of the electric and magnetic fields at all preceding moments $t' \leq t$.

The time interval $\tau = t - t'$ for which the previous history still has a significant effect is defined by the metal's characteristic frequencies ω_s . It is obvious that, for electromagnetic fields oscillating at a very high frequency $\omega \gg \omega_s$, the electrons do not have enough time to form any significant polarization and magnetization. Eventually, this results in very weak temporal dispersion with

$$\varepsilon_{ij}(\omega \rightarrow \infty) = \delta_{ij}, \quad \mu_{ij}(\omega \rightarrow \infty) = \delta_{ij}.$$

However, at frequencies ω below or close to the characteristic frequencies ω_s , the temporal dispersion increases and becomes significant.

In general, the characteristic frequencies ω_s are different for electric (ω_E) and magnetic (ω_H) properties of metals. For diamagnetic and paramagnetic metals, the magnetic characteristic frequencies ω_H usually lie far below the optical range, while the electric frequencies ω_E vary from the near infrared to the ultraviolet [2]. Therefore, most diamagnetic and paramagnetic metals lose their magnetic properties early, before reaching the optical range. Thus, starting from the optical frequencies, they feature

$$\mu_t = \mu_l = 1, \tag{1.19}$$

with the temporal dispersion given by $\varepsilon_{ij}(\omega)$.